Perspective

Earthquake energy dissipation in a fracture mechanics framework

David S. Kammer [1] ✉, Gregory C. McLaskey[2], Rachel E. Abercrombie [3], Jean-Paul Ampuero [4], Camilla Cattania[5], Massimo Cocco[6], Luca Dal Zilio [7,8], Georg Dresen [9], Alice-Agnes Gabriel [10,11], Chun-Yu Ke [12], Chris Marone[12,13], Paul Antony Selvadurai [14] & Elisa Tinti [6,13]

Earthquakes are rupture-like processes that propagate along tectonic faults and cause seismic waves. The propagation speed and final area of the rupture, which determine an earthquake's potential impact, are directly related to the nature and quantity of the energy dissipation involved in the rupture process. Here, we present the challenges associated with defining and measuring the energy dissipation in laboratory and natural earthquakes across many scales. We discuss the importance and implications of distinguishing between energy dissipation that occurs close to and far behind the rupture tip, and we identify open scientific questions related to a consistent modeling framework for earthquake physics that extends beyond classical Linear Elastic Fracture Mechanics.

Earthquakes are one of the most damaging natural hazards facing humankind. Improvements in understanding the fundamental physics of earthquakes could have dramatic consequences for our ability to plan and react to catastrophic earthquakes in densely populated areas. Seismological observations show that earthquakes comprise a rupture front propagating along a fault and leaving behind slip and stress drop, which is a form of fracture propagation. Thus the field of fracture mechanics has played a fundamental role in shaping what we know about earthquake physics. Classical models describe an earthquake as a shear crack and define, for example, the relationship between earthquake rupture area, propagation speed, and the spectral characteristics of radiated seismic waves[1–3]. While the overall energy budget that compares states before and after an earthquake has a well-established theoretical basis[4], key aspects of the instantaneous energy balance governing the behavior of the earthquake rupture remain poorly understood. Fracture mechanics theory predicts that rupture growth is a balancing act involving three components: 1) energy dissipated to extend the crack, either by creating new surface area or generating frictional heat, 2) energy radiated as seismic waves, and 3) release of stored elastic energy from the surrounding rock. This view has been confirmed by a broad range of laboratory experiments and codified in the theory of Linear Elastic Fracture Mechanics (LEFM)[5]. However, the complexity of earthquake faults far exceeds that of typical laboratory setups, raising significant questions about the applicability and predictive power of LEFM in natural conditions[6,7]. One of our goals here is to paint a picture of the state of the art in understanding earthquake rupture and, in particular, the extent to which LEFM can further our understanding of the earthquake energy budget in cases where the fault zone has finite width and rupture propagation involves branching, off-fault fracturing and other processes that go beyond the simple assumptions underlying LEFM.

[1]Institute for Building Materials, ETH Zurich, Zurich, Switzerland. [2]School of Civil and Environmental Engineering, Cornell University, Ithaca, NY, USA. [3]Boston University, Boston, MA, USA. [4]Université Côte d'Azur, Observatoire de la Côte d'Azur, IRD, CNRS, Géoazur, Valbonne, France. [5]Department of Earth, Atmospheric, and Planetary Sciences, Massachusetts Institute of Technology, Cambridge, MA, USA. [6]Istituto Nazionale di Geofisica e Vulcanologia, Rome, Italy. [7]Earth Observatory of Singapore, Nanyang Technological University, Singapore, Singapore. [8]Asian School of the Environment, Nanyang Technological University, Singapore, Singapore. [9]Helmholtz Centre Potsdam, GFZ German Research Centre for Geosciences, Potsdam, Germany. [10]Scripps Institution of Oceanography, UCSD, La Jolla, USA. [11]Ludwig-Maximilians-Universität München, Munich, Germany. [12]Department of Geosciences, The Pennsylvania State University, University Park, PA 16802, USA. [13]La Sapienza Universitá di Roma, P.le Aldo Moro 5, 00185 Roma, Italia. [14]Swiss Seismological Service, ETH Zurich, Zurich, Switzerland. ✉e-mail: dkammer@ethz.ch
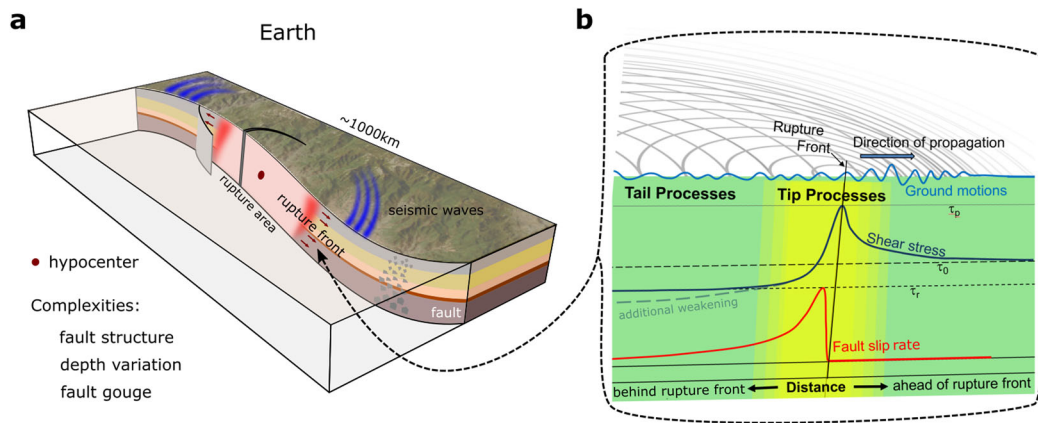
Fig. 1 | Schematic of an earthquake with its rupture front and seismic waves. **a** Earthquake fault complexity includes fault geometry, depth variation in geological units, wear and gouge formation within the fault zone, and fault branching. The red zone near the rupture front indicates regions with high fault slip rates. Note seismic waves (blue) radiate from the fault zone. **b** The evolution of the fault zone shear stress (blue) and slip rate (red) are shown for the region around the rupture tip and toward the hypocenter where the fault has already slipped. Seismic waves are indicated by gray lines and the associated ground motions are illustrated by a bright blue line. Processes within the rupture tip and in the tail behind the tip, so-called tip-and-tail processes, are a major focus of this Perspective.

While there is transformative potential in extending knowledge and connections between the fields of fracture mechanics and earthquake physics, there are several key impediments. These include: 1) a lack of fundamental understanding of how various dissipative processes at different spatial and temporal scales contribute to the mechanics of earthquakes, 2) extreme discrepancies (of many orders of magnitude) between values of fracture energy measured in laboratory experiments[8] and inferred from natural earthquakes, and 3) vastly different terminology between the communities. In this Perspective, we aim to review the mechanics and energy dissipation in earthquake ruptures, define a clear terminology, and discuss the capabilities and limitations of current observations and measurement techniques and how they affect the observed discrepancies. Finally, we propose a path forward in the form of key outstanding questions, clear scientific objectives for future work, and suggestions to overcome the limitations of LEFM as applied to earthquake faulting.

Fundamentals of theoretical earthquake mechanics

The mechanics of earthquakes are complex and arguably equally challenging to measure as to theoretically describe. The goal of a theoretical earthquake model is to describe the essential processes with viable equations and tools that allow field observation to be interpreted. Hence, it builds on common observations, which show that earthquake ruptures begin in a localized region of a fault known as the hypocenter (see Fig. 1), which is the location where initial shear stresses (τ_0) are sufficient to overcome frictional strength and the fault motion begins to accelerate. The initial stress level is one of the most difficult parameters to constrain. It can be spatially variable, and it can have a large impact on rupture style and speed. Unlike static frameworks, such as slip-tendency analysis popular in structural geology, faults can be stressed well below strength almost everywhere and yet rupture spontaneously: only a small portion of the fault needs to reach its strength to nucleate an earthquake. For ordinary earthquakes with fast rupture speeds, the hypocenter is the location where seismic waves are first radiated. From there, earthquake rupture expands along the fault, causing the fault surfaces to begin to slip. The transition region between slipping and unslipped sections of the fault is called the rupture front (see Fig. 1). For fast ruptures, moving at speeds of several km/s, the slip rate of fault surfaces accelerates from below 1 μm/s to above 1 m/s over timescales of less than a second. Ahead of the rupture front, the shear stress on the fault increases in what is called a dynamic stress concentration. At the

rupture tip, a rapid transition occurs. The slip rate increases as the shear stress drops rapidly to a dynamic level τ_d that is below the initial level τ_0. This drop in stress causes a release of stored strain energy, which drives the rupture. Simultaneously, part of this energy is dissipated through various processes, including fracture of the surrounding rock, comminution (the production of rock powders), heating, and possibly melting of rocks. The remaining energy is radiated as seismic waves that transport kinetic energy far from the source and cause ground shaking, ultimately to be dissipated as heat. Eventually, the rupture ceases to grow, and all sections of the earthquake rupture area arrest (or evolve to a very slow and long quasi-static front of postseismic slip). This can occur because continued slip necessitates a disproportionately large amount of energy dissipation or because the rupture front propagates into unfavorably stressed regions (i.e., $\tau_0 < \tau_d$).

Earthquakes as a rupture process described by fracture mechanics

The earthquake rupture process of propagation and arrest shares many features of a crack propagating through a solid material. Thus, the theoretical framework of LEFM, as summarized in Box 1, has been adapted to describe the mechanics of earthquake rupture [e.g.,[9–11]]. Specifically, under suitable assumptions, LEFM provides an energy balance that governs rupture growth:

$$G = \Gamma_{\text{tot}} , \tag{1}$$

where G is the energy release rate and Γ_{tot} the fracture energy (precise definitions are provided in Box 1). LEFM allows rupture speed prediction based on a few assumptions given in Box 1

$$C_f \approx \left(1 - \frac{\Gamma_{\text{tot}}}{G_0}\right) C_R , \tag{2}$$

where C_f is the rupture speed, C_R is the Rayleigh wave speed, and G_0 is the static energy release rate. However, the application of LEFM to earthquake ruptures requires a few key adaptions from its classical form. For instance, LEFM was initially developed for cracks that were traction-free behind the rupture front (Box 1). While valid for opening cracks, this is clearly not valid for surfaces in frictional contact. However, for many of the equations commonly used to model frictional ruptures, including rate-and-state friction equations [e.g.,[12,13]], the shear stress well behind the rupture front varies only modestly with time and position. For these cases, one can approximate the dynamic

BOX 1
Fundamentals of Linear Elastic Fracture Mechanics (LEFM)

Linear Elastic Fracture Mechanics (LEFM) is a theoretical framework to describe crack growth, originally developed with a focus on opening (Mode I) cracks[90–92]. The question of whether a crack grows or not is reduced to a comparison of two states (see Box Figure): the current state with crack (half-)length ℓ and an incremental state with crack length $\ell + d\ell$. The following assumptions are made:

1. the material surrounding the crack has predominantly linear elastic behavior,
2. dissipation is localized at the crack tip,
3. the crack surface is traction-free.

One can then express the comparison of states in terms of energies stating that the crack grows if $G_0 > \Gamma_{tot}$, where G_0 is the static energy release rate and Γ_{tot} the fracture energy[93,94]. The static energy release rate is the drop in the total potential energy Π per increment of crack length given as $G_0 = -d\Pi/d\ell$, where $d\Pi \approx (U_2 - U_1) - F$ with U_i being the stored elastic strain energy for state i (see Box Figure) and F the work done by external forces in between (e.g. gravitational). The fracture energy is the energy dissipated in the process of breaking the material per unit of crack length growth. This comparison of energies is only possible because the above-mentioned assumptions guarantee a

"separation of scale" between the global quantity G_0 driving the crack and the local quantity Γ_{tot} resisting crack growth. The key aspect of this approach is that the specific physical processes of how energy is dissipated (e.g., as decohesion, plastic work) are irrelevant as long as they are localized at the crack tip, satisfying assumption 2. They are all lumped into the parameter Γ_{tot}.

To avoid infinite stresses at the crack tip, the dissipation is often smeared out in a still-localized-enough "process zone" of size $s \ll \ell$ – an approach known as "small-scale yielding" and commonly implemented via cohesive zone models[9,10,95]. While the precise limit for small-scale yielding remains unknown, a process zone with $s \approx 0.4\ell$ may, under some circumstances, still be enough localized [see pp. 142–143 in Ref. 91].

LEFM also predicts the speed at which the crack grows[5] through an energy balance, $G = \Gamma_{tot}$, where the dynamic energy release rate $G \leq G_0$ accounts for kinetic energy being radiated away from the rupture tip. Assuming time-invariant loading (i.e., no wave reflections) and 2D or circular 3D configurations, the dynamic energy release rate can be approximated by $G \approx (1 - C_f/C_R)G_0$, where $C_f = d\ell/dt$ is the rupture speed and C_R the material Rayleigh wave speed.
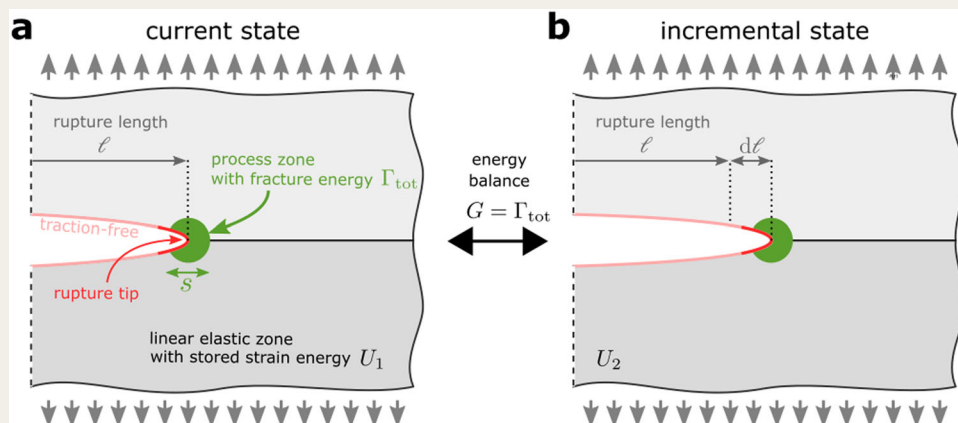
Box Figure | Schematic of the fundamental principles for crack growth in Linear Elastic Fracture Mechanics. a The current state of a material system under remote applied load (gray arrows) containing a rupture of length ℓ with a process zone (marked green) at the rupture tip. **b** The incremental state is the same system as shown in **a** but the rupture length increased by an incremental length $d\ell$.

friction as reaching a constant residual level τ_r for slip larger than a characteristic slip distance d_c. While this is inconsistent with expectations for complex natural faults, it provides a starting place for the application of LEFM and an opportunity to investigate the earthquake energy budget and rupture dynamics.

In the attempt to measure energy dissipation, the work done by the frictional stresses above the minimal stress through slip, commonly known as the "breakdown work" W_b, is measured/computed (see Box 2). If residual friction is constant and d_c is small enough, then the breakdown work is spatially localized in the process zone near the rupture tip. This would ensure the above-mentioned separation of scale that allows the application of LEFM because the energy dissipation associated with fracture propagation is determined entirely within the crack tip region and, therefore, independent of other processes on the rest of the rupture surface. In this particular case, the breakdown work is exactly equal to the associated fracture energy, i.e., $\Gamma_{tot} = W_b$ (assuming that there are no other dissipative processes).

Some important comments:

1. breakdown work ≠ fracture energy: breakdown work W_b and associated fracture energy are not *generally* equal, as commonly assumed in some literature. The breakdown work is only equal to the fracture energy under specific conditions, i.e., when there is separation of scale (see Box 1). The precise limit of separation of scale remains unknown. Since only the localized part of the breakdown work is part of the fracture energy, $\Gamma_{tot} \leq W_b$ (in the absence of other dissipative processes).
2. fracture energy and physical processes: the fracture energy Γ_{tot} governing crack growth in Eqs. (1) and (2) is the cumulative quantity that may include the effects of many processes such as work done by frictional weakening, plastic dissipation, off-fault damage, pulverization within the fault zone, and others, i.e., $\Gamma_{tot} = \sum \Gamma_{processes}$. However, Γ_{tot} only includes the part of the energy that is localized near the crack tip (on- or off-fault) to comply with separation of scale and to be consistent with LEFM.

BOX 2
The breakdown work

The breakdown work[67,96] is the measurable portion of the frictional work density, which, when integrated on the fault surface, gives an estimate of the irreversible part of the total strain energy change that does not go into radiated energy[6,8]. Ref. 67 defined the breakdown work W_b as the excess of work over the minimum shear stress achieved during slip τ_{min}:

$$W_b = \int_0^{t_b} (\tau(t) - \tau_{min}) \dot{\delta}(t) dt = \int_0^{d_c} (\tau(\delta) - \tau_{min}) d\delta \quad (3)$$

where $\dot{\delta}(t)$ is the slip rate, $\tau(t)$ the shear stress, and t_b is the time at which τ_{min} and the critical slip distance d_c are reached[97].

3. fracture energy variability: due to its multi-physical origin, the fracture energy may vary spatially along the fault and change with rupture speed. Hence, it may not be known a-priori.
4. non-localized heat: the so-called "frictional heat," e.g., $W_H = \int_0^D \tau_r d\delta$, which is the work of residual friction τ_r on the fault, is *not* included in Γ_{tot} as it is *not* localized. Consequently, the energy due to the residual stress is also excluded from G, and the Griffith energy balance (Eq. (1)). We note that while the majority of the total dissipation goes into frictional heat, this does not detract from the importance of the fracture energy for rupture propagation.

Applicability of fracture mechanics to laboratory ruptures versus natural earthquakes

Frictional stick-slip events or fracture propagation on pre-existing surfaces represent the laboratory equivalent of earthquakes. While earthquakes generated in the laboratory (so-called "labquakes") share many features of natural earthquakes[14] on tectonic faults, the vast differences in scale raise important questions that include the application of LEFM to labquakes and earthquakes on natural faults. Yet, recent works provide a useful starting point because they include quantitative predictions of rupture speed[15,16] and arrest[17–19] for labquakes. These and similar experiments also measure the fracture energy Γ_{tot} of labquakes with local dynamic shear stress measurements[20–23] and/or the stress-versus-slip relation[24,25]. Such experiments require a sample that is large compared to the process zone size and a critical length scale for rupture nucleation. For fault normal stresses of $1 - 10$ MPa this requires meter-scale rock samples[22,23] or $20 - 30$ cm sized samples composed of glassy polymer such as PMMA [e.g.,[20,26]]. Dynamic rupture can also be studied on smaller samples, at higher normal stress levels ($50 - 150$ MPa), if arrays of sensors are installed on the sample, inside a pressure vessel[27] and for cases where the fault zone contains sufficient wear material[28]. To infer rupture-related quantities, it is important to measure stress evolution on or near the fault as a rupture front propagates past the sensor location as opposed to sample-wide averages.

LEFM has also been applied to tectonic faults to examine physical processes such as aseismic slip, occurring naturally or by fluid injection [e.g.,[29–33]], the statistical properties of small earthquakes [e.g.,[34–36]], the frequency-magnitude distribution [e.g.,[37,38]], earthquake nucleation [e.g.,[9,39,40]], and for rupture propagation and arrest [e.g.,[41]]. These results demonstrate that LEFM, even with its strong simplifying assumptions, is a powerful concept to describe the fundamental mechanics of earthquakes and faults.

In summary, the simplifying assumptions of LEFM appear to be valid for large-scale laboratory experiments where LEFM quantitatively describes rupture speed and arrest. However, laboratory experiments differ from natural faults in several ways that must be accounted for to understand the limitations of LEFM and to develop appropriate extensions of that theory. First, the magnitude range of labquakes is relatively limited, which impedes a precise determination of earthquake scaling properties. Furthermore, laboratory experiments are often conducted at low stress levels (~5MPa) compared to the unconfined strength of the rock or polymer samples. This limits off-fault damage or inelastic deformation that may strongly affect the rupture process and the overall energy dissipation. The experiments also typically employ simple fault geometries, while tectonic faults are much more complex. Under some conditions, the complexities of geological faults can be lumped into a single tip-localized parameter Γ_{tot}; however, for other cases, the framework of LEFM requires modification. A key question is if energy dissipation (aside from frictional heat) on natural faults with all its complexities (e.g., weakening, off-fault inelasticity) truly is localized in the vicinity of the rupture tip, which would guarantee separation of scale and applicability of LEFM. Should this not be the case, is it enough if "most" of the energy is dissipated in a localized manner? The implications of these questions are important as the answers determine the extent to which LEFM can be applied to earthquakes in its current or modified forms.

While numerical simulations are a powerful tool to model earthquakes in complex systems, they also face significant challenges. As a result, they are not able to capture all processes at all space and time scales of the earthquake cycle and require significant further algorithmic and computational development to achieve fully realistic scenarios. Furthermore, theoretical tools such as LEFM are useful even if simulations can provide accurate results because they allow us to understand the "why" related to the obtained simulation results. This synergy can only be achieved if the theoretical model is correct and accounts for the relevant processes appropriately.

Tip or tail: spatiotemporal energy dissipation in earthquakes

Tectonic faulting complexity involves simultaneous dissipative processes during an earthquake, such as fracturing, comminution, heating, and possibly rock melting. These processes depend on the fault slip rate and the thickness of the shearing zone within the fault. Mechanisms such as flash heating [e.g.,[42]], melt lubrication [e.g.,[43]], thermal pressurization [e.g.,[44]], acoustic fluidization[45], elastohydrodynamic lubrication[33,46], off-fault deformation incurred during slow[47] or fast rupture[48–52] are among the various processes that have been proposed to explain energy dissipation during earthquakes.

These dissipative processes may influence the mechanics of earthquakes in different ways[8,53]. However, building on previous literature [[53–55], among others], we propose a conceptual picture (see Fig. 1) that distinguishes between the following key processes:

1. *Tip processes* dissipate energy near the rupture front and therefore contribute to the earthquake fracture energy that is equivalent to Γ_{tot} utilized in LEFM. The rupture tip region is characterized by intense slip accelerations (>100m/s²) and high slip velocities (>1m/s), but because it is highly transient, the associated slip is typically a relatively small fraction of the total coseismic slip.
2. *Tail processes* occur behind the rupture tip where slip acceleration is much lower. However, slip velocities may remain relatively high (~1m/s) in the wake of the rupture tip, especially for crack-like ruptures that are characterized by wide-spread slip compared to pulse-like ruptures during which only small parts of the fault slide at a given time. Therefore, the slip accumulated in the rupture *tail* can be large if the rupture continues long enough and may result from complex secondary ruptures (as observed in labquakes [e.g.,[22,56]]).

We note that a sharp boundary between the tip and tail processes likely does not exist and that some dissipative processes are affected by both tip and tail [e.g.,[57]]. The tip and tail terminology is not limited to interface processes (i.e., fault processes) but may also include dissipation in the bulk material (i.e., host rocks), consistent with the initial formulation of LEFM. The "tip" and "tail" terminology becomes specifically useful when discussing how different dissipative processes may affect different aspects of earthquake rupture propagation and arrest. For example, flash heating may be a weakening mechanism that is active as a tip process. In contrast, thermal pressurization will likely only occur as a tail process after sufficient slip has occurred [e.g.,[58]].

Laboratory experiments offer valuable insights into this problem, albeit with notable limitations. Most small-scale experiments, for instance, cannot achieve slip acceleration that is fast enough to fully emulate the loading conditions of a dynamic rupture front (i.e., tip processes), while large-scale rupture experiments do not exhibit enough slip for tail processes to become dominant. It is far from trivial to set up laboratory experiments capable of reproducing the slip values, velocities, and accelerations under realistic loading conditions representative of a propagating earthquake rupture. These challenges can be addressed with numerical simulations, which allow us to assess tip processes under non-trivial friction conditions or assess contributions by other dissipative mechanisms under limited conditions [e.g.,[48,59]]. Aside from limitations of laboratory and theoretical work, we also note that the theoretical definition of where the tip ends and the tail starts is not well defined and is likely model-dependent[57] and hence requires further investigation.

Finally, how do the tip and tail processes influence the mechanics of earthquakes? This is one of the key open questions in earthquake physics and is at the center of this Perspective. Without tail processes, LEFM shows, as outlined in Sec I, that the dissipative energy in the rupture tip, together with the energy release rate, controls rupture speed and arrest. Whether this is equally true for systems with significant tail processes and a "fuzzy" transition from tip to tail processes remains to be shown. Recent results[54,60,61] suggest that the tip processes dictate the rupture growth even in the presence of non-negligible tail dissipation. This suggests that the fracture energy is generally well defined by the tip processes and that in the considered cases[54,60,61], the tail processes do not significantly affect the energy release rate. However, the tail may become important when the earthquake propagates slowly – possibly during a slow arrest – propagates as multiple fronts, as a self-healing slip pulse[62], or in multiple sliding episodes across rough fault surfaces [e.g.,[63]]. It may also become important when considering how earthquakes prepare the fault for subsequent events. Here again, numerical simulations provide a tool to systematically study the link between tip and tail processes and the mechanics of earthquake ruptures.

In summary, defining tip and tail processes and how various dissipative processes contribute to them is crucial to a better understanding of how earthquakes propagate, arrest, and prepare the fault for subsequent events. The size of the yielding zone near the tip of a propagating rupture front is also an open question, which affects the values of inferred fracture energy, as we will discuss in the next section. Laboratory experiments and numerical simulations, best in synergistic combination, may provide crucial insight into these processes but require further development. Finally, the proposed framework needs to be applied to natural earthquakes but this requires a precise understanding of how field observations are linked to these tip and tail processes, which is another important open question.

Observations of energy dissipation in natural, laboratory, and simulated earthquakes

Given these theoretical considerations, we explore and compare observations of energy dissipation in both labquakes and tectonic earthquakes, with a focus on what this reveals about applying LEFM in earthquake physics. Estimates of Γ_{tot} and the total energy dissipation vary widely for labquakes, tectonic earthquakes, and numerical models of earthquake rupture. For instance, estimates by Abercrombie and Rice[64], which are calculated from a combination of seismically derived parameters (see Box 3), have suggested that the *average* energy dissipation in natural earthquakes ranges across multiple orders of magnitude from 10^2 to $10^7 J/m^2$. A compilation of seismologically inferred energy dissipation extends this range to $10^{-2} - 10^8 J/m^2$ [8,44], but these estimates are all highly model-dependent and subject to large, and potentially systematic, uncertainties[65]. Pseudo-dynamic earthquake modeling that infers shear stress evolution based on slip history [e.g.,[66]] yields estimates of MJ/m² for magnitudes M larger than 5[67] but commonly shows large variability along the fault plane[67–70]. Near-fault observations are used to infer constitutive parameters, such as the critical slip distance[71], which would imply large values of breakdown work or *average* energy dissipation. Other approaches based on dynamic models[72–76] that simulate spontaneous dynamic rupture and employ a frictional constitutive law yield estimates of total energy dissipation that range from 1 to 10MJ/m².

Similar estimates of energy dissipation from acoustic emission spectra of labquakes yield values of $10^{-6} - 1 J/m^2$ [77]. In more traditional shear fracture experiments of intact rock, however, the fracture energy has been measured in the range $10^3 - 10^4 J/m^2$ at the 100MPa pressures expected in much of the seismogenic crust[78–82]. This is the energy required to form a fault in intact rock and is supposed to be orders of magnitude higher than the fracture energy required to rupture an existing tectonic fault. Energy dissipation estimated from friction experiments on rough surfaces that are flat at long wavelength yield estimates of $10^{-1} - 10^1 J/m^2$ [22–25]. Other experiments where surfaces experience large slip and concentrated shear heating show continued weakening of the interface up to 1m of slip[83,84], which has been interpreted as energy dissipation up to 1MJ/m². Still, other data come from mining-induced earthquakes where the faults intersect working faces. The fraction of energy dissipated during an M2.1 mining event was estimated to be about $1 - 9\%$ of the total energy released[85,86]. More recently ref. 87 arrived at a similar fraction of <1% of the total energy based on fault gouge analysis, which corresponds to an average dissipated energy per event of roughly 0.5MJ/m².

The interpretation of the broad range of values inferred for energy dissipation (per unit area) requires careful analysis, as some may correspond to (tip-localized) fracture energy, and others correspond to energy dissipation within a broader region that is not localized and should, therefore, not be included in fracture energy. For example, quasi-static laboratory experiments, including rotary shear and other experiments with modest slip acceleration (5 m/s²), produce conditions appropriate for tail processes, not tip processes. Thus, under these conditions, the inferred dissipation does not correspond to the fracture energy and $W_b \neq \Gamma_{tot}$. Spectral seismological estimates [e.g., compilations of refs. 44,64] use information from the entire earthquake rupture area, rather than from just the propagating rupture front, and can therefore also include 'tail' dissipation mechanisms.

It has also been shown[88] that the resolution of shear stress evolution inferred from pseudodynamic modeling [e.g.,[67]] is limited by the bandwidth of the input data, either from the band limits imposed on ground motions or from smoothing operators used to regularize the kinematic finite-fault inversions. However, integral quantities such as fracture energy or breakdown work are less affected by bandwidth limitations, and thus, they are considered more reliable measures. Scale dependence of the physical processes governing dynamic weakening might also explain both the broad range of values and the scaling of energy dissipation with slip [see ref. 8 and references therein]. Given the tip-and-tail separation outlined above, future research is needed to determine the values of Γ_{tot} and the total energy

BOX 3

Seismologically derived earthquake parameters

Abercrombie and Rice[56] proposed a parameter G', here denoted W'_b to avoid confusion with energy release rate:

$$W'_b = \frac{D}{2}\left(\Delta\sigma - \frac{2\mu E_R}{M_0}\right), \tag{4}$$

where D is the average slip over the fault plane, $\Delta\sigma$ the average stress drop, μ the rock shear modulus, E_R the radiated energy, and M_0 the seismic moment. W'_b is theoretically equal to the breakdown work as long as the final stress $\overline{\tau}^E_f$ is equal to the residual sliding strength of the fault τ_r. This approach is entirely based on seismologically derived parameters and can be based on rupture averages from simple source models or derived from finite-fault modeling with spatially and temporally varying slip. The most reliable seismologically derived parameter is the seismic moment

$$M_0 = \mu AD, \tag{5}$$

where A is the rupture area. In finite-fault models, the stress drop can be determined from the spatially varying slip, but for smaller earthquakes, it is typically determined by assuming a simple circular source model[1]:

$$\Delta\sigma = \frac{7}{16}\frac{M_0}{r^3}. \tag{6}$$

For circular ruptures, r can be estimated from the corner frequency of the spectrum of teleseismic waves (f_0) or the reciprocal of the pulse duration in time domain modeling,

$$r = k\frac{C_S}{f_0}, \tag{7}$$

where k is a geometrical constant that varies widely for commonly used source models[1,3,89], and C_S is the shear wave speed. These seismologically determined source parameters are subject to large systematic and random uncertainties and should be interpreted and modeled with extreme caution[57].

dissipation retrieved at different scales and use different techniques to evaluate both laboratory data and natural earthquakes.

Several recent works have discussed the increase of fracture energy and breakdown work with total slip or earthquake size. A coherent interpretation of this scaling is still lacking, which implies that some caution is warranted. However, we note that this scaling is observed in seismological estimates from both natural earthquakes[64] and labquakes[77] as well as in numerical modeling studies, as shown in ref. [8]. On the other hand, Ke et al.[89] proposed a numerical model to suggest that scaling of seismologically estimated energy dissipation with slip can result from stress overshoot (i.e., lower final stress than dynamic friction), rather than a true increase of fracture energy with rupture size and fault slip. While overshoot cannot be used to explain the scaling reported from pseudo-dynamic modeling[67], that work raises important questions about how to reconcile the huge range of fracture energy measurements and the earthquake energy budget. This highlights the importance of further research to adjust current practices used to perform dynamic modeling of natural earthquakes and ground motion predictions.

Conclusion & outlook

This perspective discusses the earthquake energy budget and the potential of Linear Elastic Fracture Mechanics (LEFM) theory to describe earthquake rupture in the laboratory and nature. The key condition for LEFM applicability is that energy dissipation during rupture propagation (except for frictional heat) must be localized in a small-scale zone at the rupture tip – a condition that is commonly satisfied in large-scale laboratory experiments but may not be fully met for tectonic faults with all of their complexity. This raises important questions about how to consistently and correctly describe the energy dissipation of natural earthquakes. We suggest distinguishing between *tip* processes that account for localized dissipation and *tail* processes that occur further away from the rupture tip. In this framework, tip

processes govern earthquake rupture extension and propagation, while tail processes are more important for other measures of earthquake energy dissipation and the global energy budget. We also highlight the large range of measured or inferred energy dissipation from labquakes and earthquakes across many orders of magnitude and the possibility that this could result from comparing localized with non-localized dissipation.

While the proposed tip-versus-tail perspective provides a useful approach to discussing energy dissipation in earthquakes, it also opens important scientific questions that are to be addressed in future research. For instance, the boundary between the tip and tail, i.e., the localization of energy dissipation, is neither well defined nor known. Experiments and field observations with improved sensing are needed to measure the contributions to tip and tail energy dissipation. Here it is important to note that any physical process may contribute to dissipation in the tip and the tail concurrently, and hence, separating the contributions to each is required. It is also important to use precise and consistent terminology to avoid misinterpretation of data. Specifically, only rupture-tip energy dissipation should be termed "fracture energy"; and when there is no proof that energy dissipation is local to the rupture tip, more general terms, such as "breakdown work," should be used.

Another important open question concerns the effect of significant tail processes on earthquake propagation and arrest mechanisms. Do these processes affect the energy balance (Eq. (1)) and, hence the rupture speed? Here, numerical simulations are particularly useful to systematically explore and isolate these effects and to update the fracture theory for the description of rupture growth in the presence of tail processes. Such simulations could also provide a tool to determine the link between fault properties (tip and tail processes) and averaged global observations as inferred from seismological data and hence support the correct interpretation of earthquake energy dissipation across scales.

In conclusion, as a community, we need to synergistically combine field observations, laboratory experiments, and numerical simulations to determine the degree of rupture-tip localization of various energy dissipative processes and the effect of non-localized dissipation on rupture mechanics to build a consistent model for earthquake physics.

References

1. Brune, J. N. Tectonic stress and the spectra of seismic shear waves from earthquakes. *J. Geophys. Res.* **75**, 4997 (1970).
2. Boatwright, J. A spectral theory for circular seismic sources; simple estimates of source dimension, dynamic stress drop, and radiated seismic energy. *Bull. Seismolog. Soc. Am.* **70**, 1 (1980).
3. Madariaga, R. Dynamics of an expanding circular fault. *Bull. Seismolog. Soc. Am.* **66**, 639–666 (1976).
4. Kostrov, V. Seismic moment and enengy of earthquakes, and the seismic flow of rock. *Izv. Acad. Sci. USSR* **1**, 23 (1974).
5. Freund, L. B. *Dynamic Fracture Mechanics* (Cambridge University Press, 1998).
6. Kostrov, B. V. & Das, S. *Principles of Earthquake Source Mechanics* (Cambridge University Press, 1988).
7. Rudnicki, J. W. Fracture mechanics aplied to the earth's crust. *Annual Rev. Earth Planet. Sci.* **8**, 489 (1980).
8. Cocco, M. et al. Fracture energy and breakdown work during earthquakes. *Annual Rev. Earth Planet. Sci.* **51**, 217–252 (2023).
9. Ida, Y. Cohesive force across the tip of a longitudinal-shear crack and Griffith's specific surface energy. *J. Geophys. Res.* **77**, 3796 (1972).
10. Palmer, A. C. & Rice, J. R. The growth of slip surfaces in the progressive failure of over-consolidated clay. *Proc. R. Soc. Lond. Math. Phys. Sci.* **332**, 527 (1973).
11. Scholz, C. H. *The Mechanics of Earthquakes and Faulting* (Cambridge University Press, 2019).
12. Marone, C. Laboratory-derived friction laws and their application to seismic faulting. *Annual Rev. Earth Planet. Sci.* **26**, 643 (1998).
13. Leeman, J. R., Saffer, D. M., Scuderi, M. M. & Marone, C. Laboratory observations of slow earthquakes and the spectrum of tectonic fault slip modes. *Nat. Commun.* **7**, 11104 (2016).
14. Cebry, S. B. L., Ke, C.-Y. & McLaskey, G. C. The role of background stress state in fluid-induced aseismic slip and dynamic rupture on a 3-m laboratory fault. *J. Geophys. Res.: Solid Earth* **127**, e2022JB024371 (2022).
15. Svetlizky, I., Kammer, D., Bayart, E., Cohen, G. & Fineberg, J. Brittle fracture theory predicts the equation of motion of frictional rupture fronts. *Phys. Rev. Lett.* **118**, 125501 (2017).
16. Kammer, D. S., Svetlizky, I., Cohen, G. & Fineberg, J. The equation of motion for supershear frictional rupture fronts. *Sci. Adv.* **4**, eaat5622 16–37 (2018).
17. Kammer, D. S., Radiguet, M., Ampuero, J.-P. & Molinari, J.-F. Linear elastic fracture mechanics predicts the propagation distance of frictional slip. *Tribol. Lett.* **57**, 1 (2015).
18. Bayart, E., Svetlizky, I. & Fineberg, J. Fracture mechanics determine the lengths of interface ruptures that mediate frictional motion. *Nat. Phys.* **12**, 166 (2016).
19. Ke, C.-Y., McLaskey, G. C. & Kammer, D. S. Rupture termination in laboratory-generated earthquakes. *Geophys. Res. Lett.* **45**, 12 (2018).
20. Svetlizky, I. & Fineberg, J. Classical shear cracks drive the onset of dry frictional motion. *Nature* **509**, 205 (2014).
21. Bayart, E., Svetlizky, I. & Fineberg, J. Rupture dynamics of heterogeneous frictional interfaces. *J. Geophys. Res.: Solid Earth* **123**, 3828 (2018).
22. Kammer, D. S. & McLaskey, G. C. Fracture energy estimates from large-scale laboratory earthquakes. *Earth Planet. Sci. Lett.* **511**, 36 (2019).
23. Xu, S., Fukuyama, E. & Yamashita, F. Robust estimation of rupture properties at propagating front of laboratory earthquakes. *J. Geophys. Res.: Solid Earth* **124**, 766 (2019).
24. Okubo, P. G. & Dieterich, J. H. Fracture energy of stick-slip events in a large scale biaxial experiment. *Geophys. Res. Lett.* **8**, 887 (1981).
25. Okubo, P. G. & Dieterich, J. H. Effects of physical fault properties on frictional instabilities produced on simulated faults. *J. Geophys. Re.: Solid Earth* **89**, 5817 (1984).
26. Rubino, V., Rosakis, A. & Lapusta, N. Understanding dynamic friction through spontaneously evolving laboratory earthquakes. *Nat. Commun.* **8**, 1 (2017).
27. Passelègue, F. X., Schubnel, A., Nielsen, S., Bhat, H. S. & Madariaga, R. From sub-rayleigh to supershear ruptures during stick-slip experiments on crustal rocks. *Science* **340**, 1208 (2013).
28. Shreedharan, S., Bolton, D. C., Riviére, J. & Marone, C. Competition between preslip and deviatoric stress modulates precursors for laboratory earthquakes. *Earth Planet. Sci. Lett.* **553**, 116623 (2021).
29. Hawthorne, J. C. & Rubin, A. M. Laterally propagating slow slip events in a rate and state friction model with a velocity-weakening to velocity-strengthening transition. *J. Geophys. Res.: Solid Earth* **118**, 3785 (2013).
30. Garagash, D. I. Fracture mechanics of rate-and-state faults and fluid injection induced slip. *Philosoph. Trans. R. Soc. A* **379**, 20200129 (2021).
31. Dublanchet, P. Fluid driven shear cracks on a strengthening rate-and-state frictional fault. *J. Mech. Phys. Solids* **132**, 103672 (2019).
32. Galis, M., Ampuero, J. P., Mai, P. M. & Cappa, F. Induced seismicity provides insight into why earthquake ruptures stop. *Sci. Adv.* **3**, eaap7528 (2017).
33. Dal Zilio, L., Hegyi, B., Behr, W. & Gerya, T. Hydro-mechanical earthquake cycles in a poro-visco-elasto-plastic fluid-bearing fault structure. *Tectonophysics* **838**, 229516 (2022).
34. Dublanchet, P. The dynamics of earthquake precursors controlled by effective friction. *Geophys. J. Int.* **212**, 853 (2018).
35. Dublanchet, P. & De Barros, L. Dual seismic migration velocities in seismic swarms. *Geophys. Res. Lett.* **48**, e2020GL090025 (2021).
36. Cattania, C. & Segall, P. Crack models of repeating earthquakes predict observed moment-recurrence scaling. *J. Geophys. Res.: Solid Earth* **124**, 476 (2019).
37. Dempsey, D. and Suckale, J. Forecasting induced seismicity rate and Mmax using calibrated numerical models, in *AGU Fall Meeting Abstracts*, Vol. 2016 (2016) pp. S23D–04.
38. Cattania, C. Complex earthquake sequences on simple faults. *Geophys. Res. Lett.* **46**, 10384 (2019).
39. Rubin, A. M. and Ampuero, J.-P. Earthquake nucleation on (aging) rate and state faults. *J. Geophys. Res.: Solid Earth* **110** (2005).
40. Cattania, C. A source model for earthquakes near the nucleation dimension. *Bull. Seismolog. Soc. Am.* **113**, 909–923 (2023).
41. Weng, H. & Ampuero, J.-P. The dynamics of elongated earthquake ruptures. *J. Geophys. Res.: Solid Earth* **124**, 8584 (2019).
42. Rice, J. R. Heating and weakening of faults during earthquake slip. *J. Geophys. Res.: Solid Earth* **111**, B6 (2006).
43. Nielsen, S., Di Toro, G., Hirose, T., and Shimamoto, T. Frictional melt and seismic slip. *J. Geophys. Res.: Solid Earth* **113**, https://doi.org/10.1029/2007JB005122 (2008).
44. Viesca, R. C. & Garagash, D. I. Ubiquitous weakening of faults due to thermal pressurization. *Nature Geosci.* **8**, 875 (2015).
45. Melosh, H. J. Dynamical weakening of faults by acoustic fluidization. *Nature* **379**, 601 (1996).
46. Brodsky, E. E. & Kanamori, H. Elastohydrodynamic lubrication of faults. *J. Geophys. Res.: Solid Earth* **106**, 16357 (2001).

47. Rudnicki, J. & Rice, J. Conditions for the localization of deformation in pressure-sensitive dilatant materials. *J. Mech. Phys. Solids* **23**, 371–394 (1975).

48. Andrews, D. J. Rupture dynamics with energy loss outside the slip zone. *J. Geophys. Res.: Solid Earth* **110**, https://doi.org/10.1029/2004JB003191 (2005).

49. Ben-Zion, Y. & Shi, Z. Dynamic rupture on a material interface with spontaneous generation of plastic strain in the bulk. *Earth Planet. Sci. Lett.* **236**, 486 (2005).

50. Rice, J. R., Sammis, C. G. & Parsons, R. Off-Fault Secondary Failure Induced by a Dynamic Slip Pulse. *Bull. Seismological Soc. Am.* **95**, 109 (2005).

51. Bhat, H. S., Dmowska, R., King, G. C. P., Klinger, Y., and Rice, J. R. Off-fault damage patterns due to supershear ruptures with application to the 2001 Mw 8.1 Kokoxili (Kunlun) Tibet earthquake. *J. Geophys. Res.: Solid Earth* **112**, https://doi.org/10.1029/2006JB004425 (2007).

52. Gabriel, A.-A., Ampuero, J.-P., Dalguer, L. & Mai, P. M. Source properties of dynamic rupture pulses with off-fault plasticity. *J. Geophys. Res.: Solid Earth* **118**, 4117 (2013).

53. Ben-Zion, Y. and Dresen, G. A synthesis of fracture, friction and damage processes in earthquake rupture zones. *Pure Appl. Geophys.* **179**, 4323–4339 (2022).

54. Paglialunga, F. et al. On the scale dependence in the dynamics of frictional rupture: Constant fracture energy versus size-dependent breakdown work. *Earth Planetary Sci. Lett.* **584**, 117442 (2022).

55. Brantut, N., Garagash, D. I. & Noda, H. Stability of pulse-like earthquake ruptures. *J. Geophys. Res.: Solid Earth* **124**, 8998 (2019).

56. Shi, S., Wang, M., Poles, Y. & Fineberg, J. How frictional slip evolves. *Nat. Commun.* **14**, 8291 (2023).

57. Cornelio, C. et al. Determination of parameters characteristic of dynamic weakening mechanisms during seismic faulting in cohesive rocks. *J. Geophys. Res.: Solid Earth* **127**, e2022JB024356 (2022).

58. Lambert, V. & Lapusta, N. Rupture-dependent breakdown energy in fault models with thermo-hydro-mechanical processes. *Solid Earth* **11**, 2283 (2020).

59. Andrews, D. J. Rupture velocity of plane strain shear cracks. *J. Geophys. Res. (1896-1977)* **81**, 5679 (1976).

60. Barras, F. et al. The emergence of crack-like behavior of frictional rupture: Edge singularity and energy balance. *Earth Planet. Sci. Lett.* **531**, 115978 (2020).

61. Weng, H. & Ampuero, J.-P. Integrated rupture mechanics for slow slip events and earthquakes. *Nat. Commun.* **13**, 7327 (2022).

62. Heaton, T. H. Evidence for and implications of self-healing pulses of slip in earthquake rupture. *Phys. Earth Planet. Int.* **64**, 1 (1990).

63. Fang, Z. & Dunham, E. M. Additional shear resistance from fault roughness and stress levels on geometrically complex faults. *J. Geophys. Res.: Solid Earth* **118**, 3642 (2013).

64. Abercrombie, R. E. & Rice, J. R. Can observations of earthquake scaling constrain slip weakening? *Geophys. J. Int.* **162**, 406 (2005).

65. Abercrombie, R. E. Resolution and uncertainties in estimates of earthquake stress drop and energy release. *Philosoph. Trans. R. Soc. A: Math., Phys. Eng. Sci.* **379**, 20200131 (2021).

66. Mai, P. M. & Thingbaijam, K. Srcmod: An online database of finite-fault rupture models. *Seismolog. Res. Lett.* **85**, 1348 (2014).

67. Tinti, E., Spudich, P., and Cocco, M. Earthquake fracture energy inferred from kinematic rupture models on extended faults. *J. Geophys. Res.: Solid Earth* **110**, https://doi.org/10.1029/2005JB003644 (2005).

68. Bouchon, M. The state of stress on some faults of the San Andreas System as inferred from near-field strong motion data. *J. Geophys. Res.: Solid Earth* **102**, 11731 (1997).

69. Causse, M., Dalguer, L. A. & Mai, P. M. Variability of dynamic source parameters inferred from kinematic models of past earthquakes. *Geophys. J. Int.* **196**, 1754 (2014).

70. Ide, S. & Takeo, M. Determination of constitutive relations of fault slip based on seismic wave analysis. *J. Geophys. Res.: Solid Earth* **102**, 27379 (1997).

71. Kaneko, Y., Fukuyama, E. & Hamling, I. J. Slip-weakening distance and energy budget inferred from near-fault ground deformation during the 2016 M_w 7.8 Kaikoura earthquake. *Geophys. Res. Lett.* **44**, 4765 (2017).

72. Tinti, E. et al. Constraining families of dynamic models using geological, geodetic and strong ground motion data: The Mw 6.5, October 30th, 2016, Norcia earthquake, Italy. *Earth Planet. Sci. Lett.* **576**, 117237 (2021).

73. Gallovic, F., Valentova, L., Ampuero, J. & Gabriel, A. Bayesian Dynamic Finite-Fault Inversion: 2. Application to the 2016 M_w 6.2 Amatrice, Italy, Earthquake. *J. Geophys. Res.: Solid Earth* **124**, 6970 (2019).

74. Premus, J., Gallovic, F. & Ampuero, J.-P. Bridging time scales of faulting: From coseismic to postseismic slip of the M_w 6.0 2014 South Napa, California earthquake. *Sci. Adv.* **8**, eabq2536 (2022).

75. Gabriel, A.-A., Garagash, D. I., Palgunadi, K. H., and Mai, P. M. Fault-size dependent fracture energy explains multi-scale seismicity and cascading earthquakes. arXiv preprint arXiv:2307.15201 (2023).

76. Palgunadi, K. H., Gabriel, A.-A., Garagash, D. I., Ulrich, T. & Mai, P. M. Rupture dynamics of cascading earthquakes in a multiscale fracture network. *J. Geophys. Res.: Solid Earth* **129**, e2023JB027578 (2024).

77. Selvadurai, P. A. Laboratory insight into seismic estimates of energy partitioning during dynamic rupture: An observable scaling breakdown. *J. Geophys. Res.: Solid Earth* **124**, 11350 (2019).

78. Wawersik, W. R. & Brace, W. F. Post-failure behavior of a granite and diabase. *Rock Mech.* **3**, 61 (1971).

79. Wong, T.-F. & Biegel, R. Effects of pressure on the micro-mechanics of faulting in san marcos gabbro. *J. Struct. Geol.* **7**, 737 (1985).

80. Wong, T.-f Shear fracture energy of westerly granite from post-failure behavior. *J. Geophys. Res.: Solid Earth* **87**, 990 (1982).

81. Wong, T.-F. On the normal stress dependence of the shear fracture energy. In *Earthquake Source Mechanics* (American Geophysical Union (AGU), 1986) pp. 1–11.

82. Lockner, D. A., Byerlee, J. D., Kuksenko, V., Ponomarev, A. & Sidorin, A. Quasi-static fault growth and shear fracture energy in granite. *Nature* **350**, 39 (1991).

83. Nielsen, S. et al. Scaling in natural and laboratory earthquakes. *Geophys. Res. Lett.* **43**, 1504 (2016).

84. Di Toro, G. et al. Fault lubrication during earthquakes. *Nature* **471**, 494 (2011).

85. Olgaard, D. & Brace, W. The microstructure of gouge from a mining-induced seismic shear zone. *Int. J. Rock Mech. Mining Sci. Geomech. Abstr.* **20**, 11 (1983).

86. McGarr, A. Earthquake prediction: Absence of a precursive change in seismic velocities before a tremor of magnitude $3\frac{3}{4}$. *Science* **185**, 1047 (1974).

87. Chester, J. S., Chester, F. M. & Kronenberg, A. K. Fracture surface energy of the punchbowl fault, san andreas system. *Nature* **437**, 133 (2005).

88. Guatteri, M. & Spudich, P. What can strong-motion data tell us about slip-weakening fault-friction laws? *Bull. Seismolog. Soc. Am.* **90**, 98 (2000).

89. Ke, C.-Y., McLaskey, G. C. & Kammer, D. S. Earthquake breakdown energy scaling despite constant fracture energy. *Nat. Commun.* **13**, 1005 (2022).

90. Griffith, A. A. Vi. the phenomena of rupture and flow in solids. *Philosoph. Trans. R. Soc. Lond. Ser. A, Cont. Pap. Math. Phys. Char.* **221**, 163 (1921).

91. Zehnder, A. T. *Fracture Mechanics*, Vol. 62 (Springer Science & Business Media, 2012).

92. Broberg, K. B. *Cracks and Fracture* (Elsevier, 1999).

93. Irwin, G. R. Onset of fast crack propagation in high strength steel and aluminum alloys, Tech. Rep. (Naval Research Lab Washington DC, 1956).

94. Williams, M. L. On the stress distribution at the base of a stationary crack. *J. Appl. Mech.* **24**, 109–114 (1957).

95. Ohnaka, M. A constitutive scaling law and a unified comprehension for frictional slip failure, shear fracture of intact rock, and earthquake rupture. *J. Geophys. Res.: Solid Earth.* **108** (2003).

96. Cocco, M., Spudich, P., and Tinti, E. On the mechanical work absorbed on faults during earthquake ruptures. In *Earthquakes: Radiated Energy and the Physics of Faulting* (American Geophysical Union (AGU), 2006) pp. 237–254.

97. Kaneko, Y. & Shearer, P. M. Variability of seismic source spectra, estimated stress drop, and radiated energy, derived from cohesive-zone models of symmetrical and asymmetrical circular and elliptical ruptures. *J. Geophys. Res.: Solid Earth* **120**, 1053–1079 (2015).

Competing interests
The authors declare no competing interests.

Additional information
Correspondence and requests for materials should be addressed to David S. Kammer.

Peer review information *Nature Communications* thanks Allan Rubin, Lingling Ye and the other, anonymous, reviewer for their contribution to the peer review of this work.

Reprints and permissions information is available at http://www.nature.com/reprints

Publisher's note Springer Nature remains neutral with regard to jurisdictional claims in published maps and institutional affiliations.